Distributions of Measurement Error for Three-Axis Magnetic Field Meters During Measurements Near Appliances

Martin Misakian and Charles Fenimore

Abstract—Comparisons are made between the average magnetic flux density as would be measured with a three-axis coil probe and the flux density at the center of the probe. Probability distributions of the differences between the two quantities are calculated assuming a dipole magnetic field and are found to be asymmetric. The distributions allow estimates of uncertainty for resultant magnetic field measurements made near some electrical appliances and other electrical equipment.

I. INTRODUCTION

THE concern in the mid 1970s regarding health effects from exposure to electric and magnetic fields in the vicinity of power lines has shifted in recent years to health effect concerns from exposure to power frequency magnetic fields in residences, the work place, and in transportation systems [1]–[3]. The magnetic fields in these environments can be highly nonuniform, particularly near electrical equipment which contain such components as transformers, motors, and heating elements. Recently, calculations have been performed which considered the influence of the size of the magnetic field probe or sensor on the accuracy of measurements near electrical appliances [4], [5]. These calculations examined the difference between the average magnetic flux density as determined with magnetic field meters with single-axis and three-axis circular coil probes[1], and the calculated magnetic flux density at the center of the probe, B_o, assuming the field was produced by a small loop of alternating current, i.e., a magnetic dipole. The magnetic dipole field was chosen as the relevant field because to a good approximation its geometry simulates the field geometry of many electrical appliances and equipment [6]. The "average" arises as a consequence of the averaging effects of the coil probes over their cross-sectional areas when placed in a nonuniform magnetic field. The difference between the average magnetic field and B_o can be thought of as a measurement error because the center of the probe is normally considered the measurement location.

In the earlier calculations, two comparisons were made:

1) The maximum average magnetic field determined at a point by rotating a single-axis probe, B_{av1}, was compared with B_o as a function of r/a where r is the

[1] The three-axis circular coil probes referred to and considered in this paper have a common central point.

distance between the magnetic dipole and the center of the probe, and a is the radius of the probe.

2) The average resultant magnetic field, B_{av3}, determined using a three-axis probe, was compared with B_o as a function of r/a. The resultant magnetic field is defined as [7]

$$B_{av3} = \sqrt{B_1^2 + B_2^2 + B_3^2},\tag{1}$$

where B_1, B_2, and B_3 are average root-mean-square (rms) magnetic field components determined by each of three orthogonally oriented coil probes.

Comparison (1) is made because maximum magnetic field levels are often measured to characterize the magnetic field when single-axis field meters are used [7], [8]. The earlier examination of comparison (1) yielded a tabulation of the differences, ΔB_{max1}, between the maximum average magnetic field, B_{av1}, and B_o [4]. A listing of ΔB_{max1} values, in percent, as a function of r/a is reproduced in Table I. These differences can be regarded as the largest errors which can occur when single-axis magnetic field meters are used to measure the maximum magnetic field from electrical appliances. The calculated errors are approximate in the sense that the calculations assume a purely $1/r^3$ spatial dependence of the magnetic field, i.e., the size of the magnetic field source is assumed to be small compared to r. For example, the size of magnetic field deflection coils in video display terminals and televisions typically would be small compared to r at most locations in front of these appliances.

TABLE I
VALUES OF ΔB_{max1} (SINGLE-AXIS PROBE) AS FUNCTION
OF NORMALIZED DISTANCE (r/a) FROM MAGNETIC DIPOLE

r/a	ΔB_{max1} (%)
3	-14.6
4	-8.7
5	-5.7
6	-4.0
7	-3.0
8	-2.3
9	-1.8
10	-1.5
11	-1.2
12	-1.0
13	-0.9
14	-0.8
15	-0.7

The earlier examination of comparison (2) yielded the largest differences between B_{av3} and B_o, i.e., the worst case errors during measurements of the resultant magnetic field [4], [5]. This paper presents the statistical distributions of the differences between B_{av3} and B_o, ΔB_{av3}, as a function of the r/a. The statistical distribution is a consequence of the fact that in practical measurement situations, the orientation of the magnetic dipole field source and the orientation of the three-axis probe are not known. As a result, ΔB_{av3} can have many values for the same value of r/a. The distributions allow one to assign measurement uncertainties arising from the averaging effects of the probe as well as to combine them with other sources of measurement error. The most probable value (or mode) of ΔB_{av3} is the most probable error and is considered later as a means for determining corrections for measurements of the resultant magnetic field. However, such corrections are found to be generally undesirable.

II. EXPRESSION FOR AVERAGE RESULTANT MAGNETIC FLUX DENSITY

The derivation of an expression giving the average magnetic flux density for a circular coil probe for arbitrary position and orientation of the probe in the dipole magnetic field is given in reference [5]. Only a brief outline is presented here. It is assumed that the cross-sectional areas of the wire in the coil probes and the opposing magnetic fields produced by currents induced in the probes are negligible. We also assume that the three orthogonally oriented coils of the three-axis probe have circular cross sections of equal area. These assumptions either can be met in practice or can be taken into account by a calibration process.

Fig. 1 shows a small alternating current loop at the origin of a Cartesian coordinate system x, y, z, and a sketch of the three-axis probe. Without loss of generality, the center of the probe is located at x_o, z_o in the x-z plane and coincides with the center of the prime coordinate system x', y', and z'. The coil probes are labeled P1, P2, and P3, have unit normal vectors n_1, n_2, and n_3, respectively, and are shown in Fig. 1 (inset) for illustrative purposes as being in the directions of prime coordinates. The orientation of the magnetic dipole with respect to the position of the probe is characterized by the angle θ, and the distance between the dipole to the center of the probe is, as indicated earlier, r.

The average magnetic flux density, B_{av}, for a single circular coil probe with cross-sectional area A is given by

$$B_{av} = \frac{1}{A} \iint_A \mathbf{B} \cdot \mathbf{n} \, dA \tag{2}$$

where dA is an element of probe area, $\mathbf{n}$ is a unit vector perpendicular to A, and $\mathbf{B}$ is the magnetic flux density.

The magnetic flux density due to the dipole is, in Cartesian coordinates [4],

$$\mathbf{B} = \mathbf{i}\frac{3Cxz}{2r^5} + \mathbf{j}\frac{3Cyz}{2r^5} + \mathbf{k}\frac{C}{2r^3}\left(\frac{3z^2}{r^2} - 1\right) \tag{3}$$

where $r = [x^2 + y^2 + z^2]^{1/2}$, $\mathbf{i}, \mathbf{j}$, and $\mathbf{k}$ are unit vectors for the Cartesian coordinates, and C is the constant $\mu_o I b^2 / 2$, μ_o is the
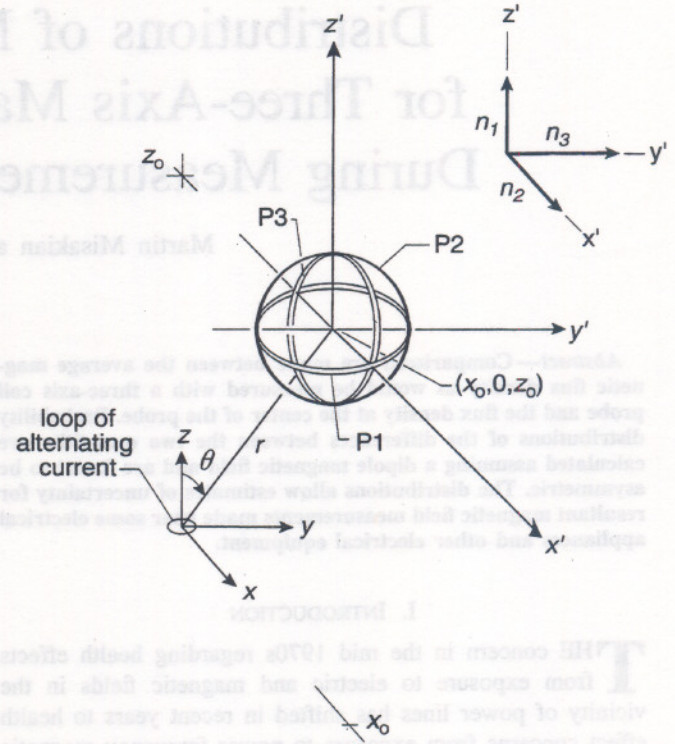

Fig. 1. Three-axis magnetic field probe with its center at $x = x_o, y = 0$, and $z = z_o$. A small current loop producing a dipole magnetic field is located at the origin of the unprimed coordinate system. The unit vectors n_1, n_2, and n_3 are normal to the areas of probes P1, P2, and P3, respectively. Changes in the angle θ correspond to varying the orientation of the dipole with respect to the probe.

permeability of vacuum, I is the alternating current, and b is the radius of the current loop. It is assumed that $b \ll r$, and the sinusoidal time dependence of the field has been suppressed. The value of B_o is given by the magnitude of $\mathbf{B}$ (3) and has axial symmetry about the z-axis.

The goal is to develop an expression for B_{av} at an arbitrary point and with arbitrary orientation. The value of B_{av3} can then be found by combining three values of B_{av} from three orthogonal directions according to (1). The approach used to obtain the desired expression for B_{av} was to transform the terms in the integrand of (2) into the coordinate system of the coil probe [5]. In this coordinate system, the unit vector normal to the plane of the coil coincides with the "z-axis," $\mathbf{B}$ is expressed in terms of the probe coordinates, and the integration is carried out numerically in polar coordinates using a double Simpson's rule. Details of the coordinate transformations which transform x, y, and z into the Cartesian probe coordinates x''', y''', and z''' are given in Ref. [5]. The relationships between coordinates in the two systems are

$$x = x_o + (z''' \sin\alpha_1 + x''' \cos\alpha_1)\cos\alpha_2 - y''' \sin\alpha_2$$
$$y = (z''' \sin\alpha_1 + x''' \cos\alpha_1)\sin\alpha_2 + y''' \cos\alpha_2$$
$$z = z_o + z''' \cos\alpha_1 - x''' \sin\alpha_1 \tag{4}$$

where α_1 and α_2 refer to angles made by the unit vector with respect to the prime coordinate system. Equation (4) is simplified by noting that the integration over the area of the
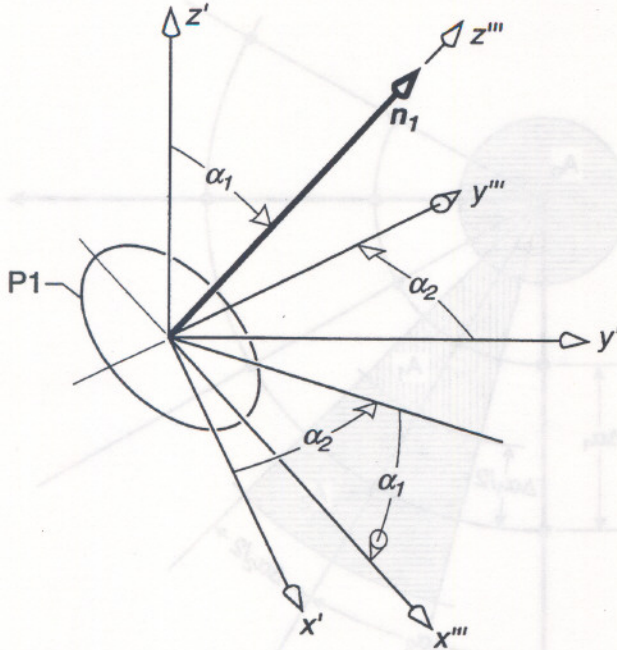
Fig. 2. Geometry of unit vector $\mathbf{n}_1$ and probe coordinates after rotation of the prime coordinates through angles α_1 and α_2. Unit vectors $\mathbf{n}_2$ and $\mathbf{n}_3$ are not shown for purposes of clarity, but retain their orthogonal relationship with $\mathbf{n}_1$.

probe (2) occurs in the plane $z''' = 0$. Fig. 2 shows the angles α_1 and α_2 for the unit vector $\mathbf{n}_1$ associated with probe P1 and the probe coordinates. Unit vector $\mathbf{n}_1$ is given by the expression [5]

$$\mathbf{n}_1 = \mathbf{i}\sin\alpha_1\cos\alpha_2 + \mathbf{j}\sin\alpha_1\sin\alpha_2 + \mathbf{k}\cos\alpha_1. \quad (5)$$

When (4) and (5) are substituted into (2), B_{av} for probe P1 can be calculated for arbitrary α_1 and α_2. Contributions to B_{av3} from the remaining two probes, P2 and P3, are obtained by using their unit vectors

$$\mathbf{n}_2 = \mathbf{i}\sin(\alpha_1 + 90°)\cos\alpha_2 + \mathbf{j}\sin(\alpha_1 + 90°)\sin\alpha_2$$
$$+ \mathbf{k}\cos(\alpha_1 + 90°)$$
$$= \mathbf{i}\cos\alpha_1\cos\alpha_2 + \mathbf{j}\cos\alpha_1\sin\alpha_2 - \mathbf{k}\sin\alpha_1 \quad (6)$$

and

$$\mathbf{n}_3 = \mathbf{n}_1 \times \mathbf{n}_2$$
$$= -\mathbf{i}\sin\alpha_2 + \mathbf{j}\cos\alpha_2 \quad (7)$$

in (2). As noted earlier, the integration for each probe is carried out numerically in polar coordinates, i.e.,

$$x''' = \rho\cos\psi, 0 \le \rho \le a, 0 \le \psi < 2\pi$$
$$y''' = \rho\sin\psi$$
$$dA = dx'''dy''' = \rho\, d\rho\, d\psi \quad (8)$$

where a is the radius of the probe.

The accuracy of the numerical integrations was checked by increasing the number of divisions between the limits of integration for ρ and ψ. The results reported below were not affected by further refinements of the intervals used during the integrations.

III. DISTRIBUTIONS OF ΔB_{av3} VALUES

In determining the distribution of ΔB_{av3} values, it is assumed that all orientations of the magnetic dipole, characterized by the angle θ, and all orientations of the three-axis probe, characterized by the unit vectors $\mathbf{n}_1, \mathbf{n}_2$, and $\mathbf{n}_3$ have equal probability. This assumption is made because, as noted earlier, during most measurement situations, the orientations of the magnetic dipole and three-axis probe typically are not known. The distribution of ΔB_{av3} values is first approximated by sampling from the parameter space $\theta, \alpha_1, \alpha_2$, and a fourth angle describing rotations about the unit vector $\mathbf{n}_1$. In algorithmic form the following sampling protocol is employed:

i) For a given probe radius a and distance r from the dipole, and with $\theta = \alpha_1 = \alpha_2 = 0$, the three-axis probe is rotated about the z'''-axis or $\mathbf{n}_1$ direction in 2° steps. The value of B_{av} for each coil probe is evaluated and combined according to (1) to obtain B_{av3} after each rotation. For each value of B_{av3}, the difference in percent from B_o is calculated and stored in computer memory. Because of the symmetry of the problem, a total rotation of 90° about the z'''-axis is required to cover all the cases without duplication. A detailed discussion of how the α values change in the integrand of (2) for each probe during rotations about the z'''-axis in this and the following steps is given in reference [5].

ii) The angle α_1 is advanced in 5° steps, and the above comparisons are repeated as the probe is rotated about the z'''-axis or $\mathbf{n}_1$ direction. The maximum value of α_1, without duplication of results is 90°.

iii) For each value of α_1, α_2 is incremented from 0° in steps of 5°, and the above comparisons are repeated. Because of symmetry arguments, a total rotation about $\mathbf{n}_1$ of 180° is required to consider all the cases without duplication.

iv) Following the above calculations, different orientations of the magnetic dipole are considered by changing the angle θ in 5° increments and repeating steps (i) through (iii). The maximum value of θ without duplication of results is 90°.

v) Steps (i) through (iv) are repeated for different values of r.

The 5° angular increments and the two-degree rotations about the z'''-axis provide enough results to determine the most probable values of ΔB_{av3} and the extremes of the distributions for different r/a values.

A diagram schematically indicating several positions for $\mathbf{n}_1$, and rotations about $\mathbf{n}_1$, as the above protocol was carried out for a fixed value of r is shown in Fig. 3. Unit vectors $\mathbf{n}_2$ and $\mathbf{n}_3$ are not shown for purposes of clarity but maintain their orthogonal relationships with $\mathbf{n}_1$.

To obtain a more accurate representation of the ΔB_{av3} distribution, it must be recognized that the points that are sampled are not uniformly distributed. That is, the frequency of calculation for the different values of ΔB_{av3} using the above protocol excessively weights the calculations for smaller values of α_1 and θ. For example, as the α values are varied and the unit vector $\mathbf{n}_1$ moves about the surface of the unit quarter-sphere with rotations (Fig. 3), it should be centered in regions of equal area so that all directions have equal
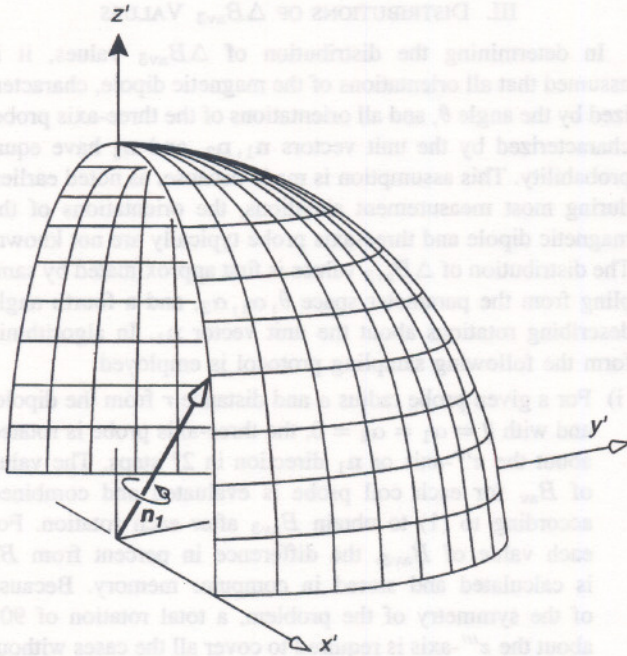
Fig. 3. Locations of n_1 during calculations of ΔB_{av3}. For each value of α_1, α_2, and θ, one degree of freedom remains, namely rotation about n_1. This rotation is carried out in two-degree steps. The unit vectors n_2 and n_3 are not shown but maintain their orthogonal relationship with n_1 as rotations about n_1 are performed.

Fig. 4. Simplified projection of portion of unit quarter sphere onto x'-y' plane. The ● indicate locations where ΔB_{av3} are calculated. For the calculations described in the text, the increments in α_1 and α_2 ($\Delta\alpha_1, \Delta\alpha_2$) are each 5° and not as shown in the figure.

probability of being considered for the calculations. However, the protocol described above calls for 5° increments in α_1 and α_2. Thus, as readily seen in the simplified projection of a portion of the unit sphere onto the x'-y' plane in Fig. 4, the surface area about each location where a calculation is performed decreases as α_1 decreases, i.e., $A_1 < A_2$ in Fig. 4. It is readily shown that the surface area about each calculation point is proportional to $\sin \alpha_1$. Thus, compared to the frequency of calculations performed when $\alpha_1 = 90°$ ($0 \leq \alpha_2 \leq 180°$), the relative frequency of calculations when α_1 is less than 90° goes as $\sin 90° / \sin \alpha_1$ or $1/\sin \alpha_1$ which is always greater than one. To correct for this "oversampling" on the unit quarter sphere for $\alpha_1 < 90°$, the occurrence of the ΔB_{av3} values must be weighted (multiplied) by $\sin \alpha_1$, and the distributions of ΔB_{av3} reported below include this correction. The one exception to this weighting procedure occurs when $\alpha_1 = 0$. The surface area on the unit hemisphere about this point is circular (Fig. 4) and is readily calculated to be 0.786 as large an area as areas about points when $\alpha_1 = 90°$ for a fixed value of r is shown in Fig. 3. Unit vec-

Similar considerations apply for the excessive frequency of ΔB_{av3} calculations for constant r and $\theta \leq 90°$. Because of the axial symmetry of the dipole magnetic field, the relevant surface area for each calculation is given by a band 5° "wide" in the angle θ on a spherical surface with radius r. The surface bands are concentric about the magnetic dipole axis (z-axis in Fig. 1). The relative areas of these bands also increase as a sine function, i.e., $\sin \theta$. This leads to a second multiplicative weighting factor, $\sin \theta$, which must be applied to the occurrence of the ΔB_{av3} values. The relative surface areas when $\theta = 0°$ and 90° are calculated to have a ratio of 0.01.
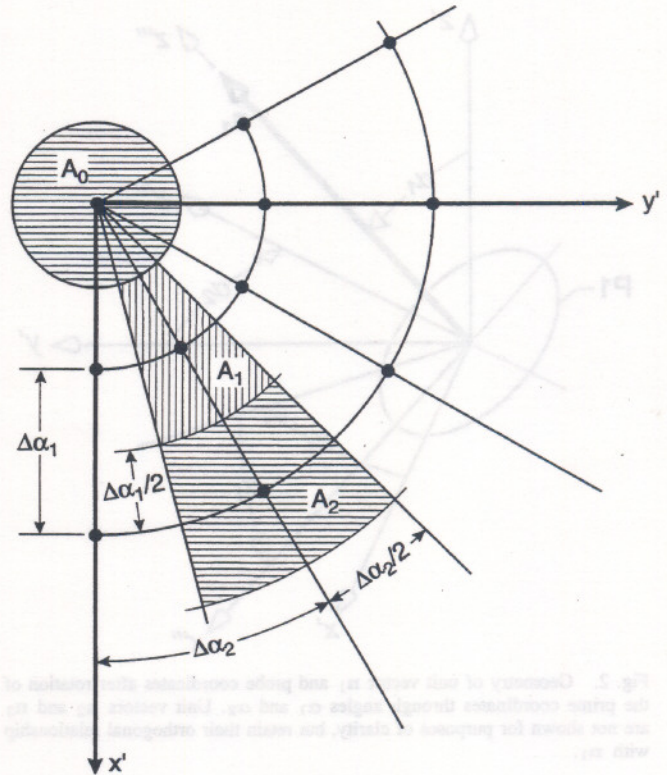
Examples of distributions of ΔB_{av3}, i.e., the weighted occurrence of ΔB_{av3} values as a function of percentage intervals, are shown as histograms in Figs. 5 and 6 for $r/a = 3$ and 8. The distributions in Figs. 5 and 6 are typical in the sense that the most probable values are positive, and the maximum negative values exceed the maximum positive values of ΔB_{av3} in magnitude. As r/a increases and the magnetic field becomes more uniform, the distributions become more narrow and the most probable value of ΔB_{av3} approaches zero, i.e., the resultant magnetic field approaches B_o, as it should. The most probable errors are taken to be the midpoints of the highest peaks in the histograms. The uncertainty introduced by this procedure is less than a 0.1% interval along the abscissa. The extreme values of ΔB_{av3} listed in Table II were determined during the calculations and saved in computer memory.

The most probable values of ΔB_{av3}, the probability or confidence intervals (CI) of 68% and 95%, and the extreme values of the ΔB_{av3} distributions are listed in Table II. The 68% confidence interval, which in the case of a normal distribution is ± one standard uncertainty (one standard deviation), is determined by calculating the 16th and 84th percentiles of the ΔB_{av3} cumulative probability distribution for each r/a. Similarly, the 95% confidence interval, normally associated with two standard uncertainties (two standard deviations) is determined by calculating the 2.5 and 97.5 percentiles. The percentages in Table II have been rounded off to the nearest 0.1% point.
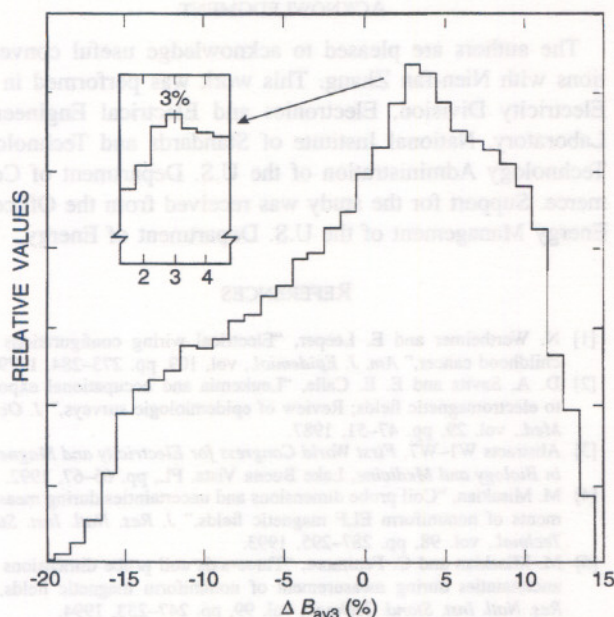
Fig. 5. Distribution of ΔB_{av3} values for $r/a = 3$. The inset shows the distribution near the most probable value with smaller percentage intervals along the abscissa.
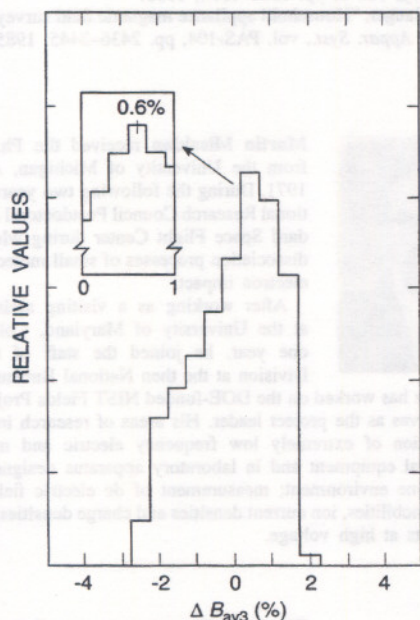

Fig. 6. Distribution of ΔB_{av3} values for $r/a = 8$. The inset shows the distribution near the most probable value with smaller percentage intervals along the abscissa.

IV. DISCUSSION

Because the distributions of measurement error are asymmetric, the common measures of central tendency (the mean, median, and mode) do not coincide for our results, and the common measure of spread in the data (the standard deviation) does not have the customary interpretation in determining confidence in a measurement. The calculated distributions of ΔB_{av3} indicate that the mode (the most probable error) is the

TABLE II
DATA FOR ΔB_{av3} PROBABILITY DISTRIBUTIONS

r/a	Most Probable Value (%)	Extreme Values (%)	68% CI (%)	95% CI (%)
3	3.0	-19.6/14.4	-8.6/8.6	-14.9/12.4
4	2.0	-10.8/7.6	-5.0/4.7	-8.6/6.7
5	1.4	-6.9/4.7	-3.3/3.0	-5.6/4.2
6	1.0	-4.8/3.2	-2.3/2.1	-3.9/2.9
8	0.6	-2.7/1.8	-1.3/1.2	-2.2/1.6
10	0.4	-1.7/1.1	-0.8/0.7	-1.4/1.0
15	0.2	-0.8/0.5	-0.4/0.3	-0.6/0.5

measure of central tendency most affected by the asymmetry. It is typically small if all orientations of the probe and dipole field are equally likely. For $r/a \geq 3$, the most probable error is 3% or less. However, the extreme values of ΔB_{av3} can be relatively large for small r/a, and the results presented in this paper can explain discrepancies between measurements at a given location with probes of the same size but with different orientations. For example, when $r/a = 3$, two "identical" accurately calibrated three-axis field meters could give readings at the same location that differ from the actual value, B_o, by -19.6% to 14.4% (this situation occurs when θ equals $90°$; note that B_o is a function of θ as well as r). The results in Table II could also help to explain discrepancies between measurements at the same location with probes of different size.

Normally there will be other sources of error, and estimates can be made of the total uncertainty using the above results. A rough estimate of the total standard uncertainty (standard deviation or 68.3% confidence interval), CI_{68}, for the error distribution when $r/a = 3$ would be

$$CI_{68} \approx -\sqrt{(-8.6)^2 + \sigma_t^2}, +\sqrt{(8.6)^2 + \sigma_t^2} \qquad (9)$$

where -8.6 and 8.6 are taken from Table II, and σ_t^2 is the variance of all other independent sources of uncertainty.

An estimate of the expanded uncertainty of "two sigma" or 95.4% confidence interval is given by

$$CI_{95} \approx -\sqrt{(-14.9)^2 + (2\sigma_t)^2}, +\sqrt{(12.4)^2 + (2\sigma_t)^2}. \quad (10)$$

The uncertainties also are estimates to the extent that r can be well determined, and the measurement location is not too close to the magnetic field source ($b \ll r$ is not satisfied), in which case the field will vary less rapidly than $1/r^3$.

Consideration was given to using the error distributions to determine correction factors for resultant magnetic field measurements. For example, the most probable error when $r/a = 3$ is 3%. This might suggest that all magnetic field measurements be "corrected" by dividing the readings by 1.03 when r/a equals 3. However, closer examination of the problem reveals that the error associated with nearly half of the measurements would be made worse (about half would be improved) by this process. Similarly, using "correction factors" determined by considering the mean or median errors also leads to adverse effects on roughly half of the measurements. If we demand that application of a correction factor should improve (or not worsen) the accuracy of all or most

measurements, this would rule out each of the above three approaches.

Alternatively, one could weaken the above requirement, demanding only that the application of a correction factor should produce a mean squared error (m.s.e.) of the corrected distribution which is less than that of the original distribution. For each of the three corrections to the mode, to the mean, and to the median, we computed the m.s.e. for the distribution for $r/a = 3$. In the case of the mode, the correction increases the m.s.e. by more than 5%, while for both the mean and the median, the m.s.e. of the corrected distribution is decreased by less than 1%. In each case, applying the "correction" either degrades the reliability of the measurement or provides marginal improvement as measured by the mean squared error.

Therefore, we recommend that no "corrections" be applied to the field values affected by the averaging and orientation effects discussed in this paper. Rather, the measurements should be reported with an indication of the total measurement uncertainty determined by combining the confidence intervals provided in Table II with other sources of uncertainty according to (9) and (10).

As a final note, the results in Table II can also be used for guidance in selecting the size of a probe for measurement environments where the field geometry is expected to be that of a dipole and highly nonuniform. For example, if the resultant magnetic field is to be measured at a distance r from a dipole source with a standard uncertainty of less than 5%, magnetic field meters with three-axis probes having radii a such that $r/a \leq 3$ would be unsuitable. Three-axis probes having radii such that $r/a \geq 5$ would be suitable if the standard uncertainty from other independent sources of uncertainty amounted to 3.7% or less, i.e.,

$$CI_{68} \approx - \sqrt{(-3.3)^2 + (3.7)^2} = -5.0\%$$
$$+ \sqrt{(3.0)^2 + (3.7)^2} = 4.8\%$$

where −3.3 and 3.0 are taken from Table II for $r/a = 5$.

V. CONCLUSION

Calculations have been performed of the probability distribution of errors (ΔB_{av3}) that can occur when magnetic field meters with three-axis circular coil probes are used to measure the resultant magnetic field produced by a miniature magnetic dipole. Because the magnetic dipole field approximates fields produced by many electrical appliances, the results may be helpful in explaining discrepancies in resultant magnetic field measurements at a given location because of differences in probe orientation or size. Knowledge of the 68% and 95% confidence intervals of the asymmetric error distribution allows one to assign estimates of uncertainties associated with the measurements.

REFERENCES

[1] N. Wertheimer and E. Leeper, "Electrical wiring configurations and childhood cancer," *Am. J. Epidemiol.*, vol. 109, pp. 273–284, 1979.
[2] D. A. Savitz and E. E. Calle, "Leukemia and occupational exposure to electromagnetic fields; Review of epidemiologic surveys," *J. Occup. Med.*, vol. 29, pp. 47–51, 1987.
[3] Abstracts W1–W7, *First World Congress for Electricity and Magnetism in Biology and Medicine*, Lake Buena Vista, FL, pp. 65–67, 1992.
[4] M. Misakian, "Coil probe dimensions and uncertainties during measurements of nonuniform ELF magnetic fields," *J. Res. Natl. Inst. Stand. Technol.*, vol. 98, pp. 287–295, 1993.
[5] M. Misakian and C. Fenimore, "Three-axis coil probe dimensions and uncertainties during measurement of nonuniform magnetic fields," *J. Res. Natl. Inst. Stand. Technol.*, vol. 99, pp. 247–253, 1994.
[6] D. L. Mader and S. B. Peralta, "Residential exposure to 60-Hz magnetic fields from appliances," *Bioelectromagnetics*, vol. 13, pp. 287–301, 1992.
[7] IEEE Magnetic Fields Task Force, "A protocol for spot measurements of residential power frequency magnetic fields," *IEEE Trans. Power Delivery*, vol. 8, pp. 1386–1394, 1993.
[8] J. R. Gauger, "Household appliance magnetic field survey," *IEEE Trans. Power Appar. Syst.*, vol. PAS-104, pp. 2436–2445, 1985.
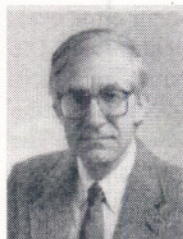
Martin Misakian received the Ph.D. in physics from the University of Michigan, Ann Arbor, in 1971. During the following two years he was a National Research Council Postdoctoral Fellow at Goddard Space Flight Center during which he studied dissociation processes of small molecules following electron impact.

After working as a visiting assistant professor at the University of Maryland, College Park, for one year, he joined the staff of the Electricity Division at the then National Bureau of Standards. Dr. Misakian has worked on the DOE-funded NIST Fields Project since 1975 and now serves as the project leader. His areas of research interest include: characterization of extremely low frequency electric and magnetic fields near electrical equipment and in laboratory apparatus designed to simulate the power line environment; measurement of dc electric fields with space charge, ion mobilities, ion current densities and charge densities; and electrical measurements at high voltage.

Charles Fenimore received the B.S. in mathematics from Union College, Schenectady, NY, and the Ph.D. in mathematics in 1979 from the University of California, Berkeley.

Since 1983, he has held a position as an applied mathematician in the Electricity Division at the National institute of Standards and Technology, Gaithersburg, MD. His research interests include nonlinear behavior in fields, in electrically driven flows, and in power systems. He is also active in image and video processing, particularly in the measurement of video quality.